Beam Squint Inspired Multiple Access Technique in Massive MIMO Systems

Abuu B. Kihero*, Liza Afeef*, and Hüseyin Arslan*

*Department of Electrical and Electronics Engineering, Istanbul Medipol University, Istanbul, 34810 Turkey Email: {abuu.kihero, liza.shehab}@std.medipol.edu.tr, huseyinarslan@medipol.edu.tr

Abstract—Massive multiple-input multiple-output (mMIMO) systems implementing wideband signaling have been found to suffer from beam squinting problem. In multicarrier systems, beam squint causes spreading of the beam to multiple undesired directions, thereby degrading system capacity. This paper proposes user scheduling and precoding techniques that controls and exploit the beam squinting phenomenon to serve multiple users and improve the overall system capacity. The proposed techniques are based on the lens antenna subarray (LAS) mMIMO system. The proposed system design is explained and numerically evaluated in terms of beam gain and capacity with different number of users and RF chains. The simulation results exhibit significant performance enhancement in terms of beam gain and capacity, corroborating the idea of exploiting the beam squinting phenomenon to serve multiple spatially separated groups of users.

Index Terms—Beam squint effect, analog subband filter, lens antenna subarray (LAS), massive MIMO, mMTC, multiple access, ultra-wideband (UWB) transmission.

I. INTRODUCTION

Massive multiple-input multiple-output (mMIMO) and ultra wideband (UWB) transmission have been considered among the candidate technological enablers for enhancing the performance and efficiency of the next-generation wireless networks. mMIMO can improve spectrum and energy efficiency, combat small scale fading through channel hardening, and extend network coverage by overcoming the path loss (PL) problem [1]. UWB transmission not only enables high data rate communication but also provides covertness against jamming attacks as in the physical layer security concept [2]. mMIMO and UWB also provide fine spatial and temporal multipath resolvability which facilitates accurate localization and ranging of target objects.

Despite these desirable advantages, it has been shown that mMIMO systems implementing UWB signaling experience a spatial-wideband effect. The Huygens-Fresnel wave propagation principle dictates that, in the antenna array systems, unless the incident signal is perpendicular to the array, the received signal at different array elements is a slightly delayed version of the original signal. The amount of delay incurred across the elements depends on the inter-element spacing and the signal's angle of arrival (AoA)/angle of departure (AoD). For a system with a relatively small number of antennas, as it is in the conventional multiple-input multiple-output (MIMO) systems, the maximum delay across the antenna aperture can be much smaller than the symbol duration, and thus its effect can be

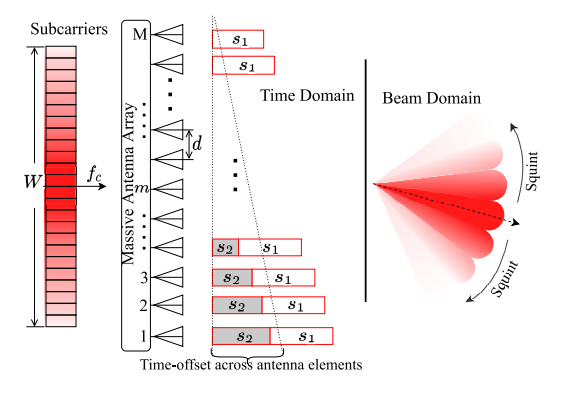


Fig. 1: Illustration of the spatial-wideband effect in time and spatial domain. ignored. However, with high-dimensional antenna arrays, i.e., mMIMO, with UWB signaling, this delay can be in the order or even larger than the symbol duration, leading to delay squinting effect in the spatial-delay domain, i.e., significant delay spread is observed across the array even in the pure line-of-sight (LoS) propagation condition. The delay squinting problem renders the steering vector frequency-dependent in the angular-frequency domain. That is, in multicarrier systems like orthogonal frequency division multiplexing (OFDM), signals at different subcarriers will point to different physical directions. Signals pertained to such derailed subcarriers might not arrive at the intended receiver or align with sidelobes or nulls of the receiver's radiation pattern, thereby degrading the performance. This phenomenon is referred to as beam squinting [3] and it is illustrated in Fig. 1.

Numerous approaches have been proposed in the literature to deal with the beam squinting problem. These approaches mostly rely on codebook based precoding [4]-[6] or digital precoding [7], [8] to minimize the beam quint. Owing to the fact that the beam squint problem is related to the analog nature of UWB signals, the above approaches only achieve minimal improvement in both array gain and spectral efficiency. Consequently some recent studies such as [9] and [10] have approached the problem from analog design perspective. Considering the fact that beam squinting involves the spatial spreading of beams as a function of subcarrier frequencies, the study in [11] set forth to the idea of exploiting this phenomenon to serve multiple, spatially distributed users. Although the idea of exploiting beam squinting to serve multiple users is quite promising, especially for the massive machine type communication (mMTC) services in which multiple users

with moderate bandwidth requirements need to be served simultaneously, more efficient ways of implementing it are still required. For example, the work in [11] does not utilize any control mechanism to ensure that all squinted beams pertaining to the intended user's subcarriers are directed to that user. This may greatly impact the achievable throughput.

To this end, this study presents a multiple access technique through a controlled beam squinting mechanism with both single and multi radio-frequency (RF) chains architectures. The proposed technique leverages our subband-based beam squinting control mechanism discussed in our previous work in [10]. The technique employs a lens antenna subarray (LAS) mMIMO architecture introduced in [12], [13] incorporated with subband filters and switches to facilitate beam squinting control in the analog domain. The available bandwidth is chunked into a number of subbands and each or several subbands are assigned to different users. The size of the subbands is adjusted such that the subcarriers within each subband result in relatively the same amount of squinting. The average squinting due to each subband is then tweaked, i.e., increased or reduced with respect to the original beam direction, to redirect the squinted beams to the locations of the intended user. This procedure is tantamount to creating multiple beams in different directions from a single beam by inducing a controllable beam squinting phenomenon. This allows us to serve multiple users with moderate to low data rate requirement as in the case of mMTC services or Internetof-Things (IoT) devices. With the proposed technique, a group of users can be simultaneously served with single RF chain. In the case of multiple RF chains, more groups of users can be simultaneously served, thereby enhancing the overall system capacity.

The rest of the paper is organized as follows: section II revises the beam squint model and its impact on the system capacity. Section III and IV give detailed description of the proposed technique for single and multi RF chains. Numerical results and conclusion are presented in section V and VI, respectively.

II. BEAM SQUINT MODEL AND ITS IMPACT

A. Channel Model

A mMIMO system with a base station (BS) equipped with M-antennas uniform linear array (ULA) is considered. Suppose there are L_p channel paths arriving at the BS where each path $\ell \in \{1,2,\ldots,L_p\}$ is associated with a passband complex gain α_ℓ , AoA/AoD $\hat{\theta}_\ell \in [-\pi/2,\pi/2)$, and the propagation delay $\tau_\ell \in [0,\tau_{\max}]$, where τ_{\max} is the channel's maximum delay spread. As briefly mentioned in Section I, for a mMIMO system implementing a very wideband signaling, there exists a non-trivial amount of delay across the array elements (with respect to the first element), given by [3]

$$\Delta \tau_{m,\ell} = (m-1) \frac{d \sin \hat{\theta}_{\ell}}{c} \tag{1}$$

with $d=\lambda_c/2$ being inter-element spacing where λ_c is the carrier wavelength, and $m\in\{1,2,\ldots,M\}$. Consequently, the total delay of an ℓ^{th} path observed by m^{th} element can

be given as

$$\tau_{m,\ell} = \tau_{\ell} + \Delta \tau_{m,\ell}. \tag{2}$$

Accordingly, the channel impulse response (CIR) observed by the m^{th} element is given as

$$h_m(t) = \sum_{\ell=1}^{L_p} \alpha_\ell e^{-j2\pi f_c \tau_{m,\ell}} \delta(t - \tau_{m,\ell}), \tag{3}$$

where f_c is the carrier frequency. Taking the Fourier transform of (3) and simplifying, the channel frequency response (CFR) of the considered link is presented as [3]

$$h_m(f) = \sum_{\ell=1}^{L_p} \tilde{\alpha}_{\ell} e^{-j2\pi(m-1)\frac{d\sin\hat{\theta}_{\ell}}{\lambda_c}} \underbrace{e^{-j2\pi(m-1)\frac{fd\sin\hat{\theta}_{\ell}}{c}}}_{\text{squint-inducing term}} e^{-j2\pi f\tau_{\ell}},$$
(4)

where $\tilde{\alpha}_\ell = \alpha_\ell e^{-j2\pi f_c \tau_\ell}$ is the equivalent baseband path gain. Stacking the channels from all M antennas, the CFR vector over the whole array can be expressed as

$$\mathbf{h}(f) = \sum_{\ell=1}^{L_p} \tilde{\alpha}_{\ell} \underbrace{\mathbf{a}_{\text{ideal}}(\hat{\theta}_{\ell}) \odot \mathbf{a}_{\text{squint}}(\hat{\theta}_{\ell}, f)}_{= \mathbf{a}(\hat{\theta}_{\ell}, f)} e^{-j2\pi f \tau_{\ell}}, \quad (5)$$

$$\mathbf{a}(\hat{\theta}_{\ell}, f) = \left[1, e^{-j2\pi(f + f_c)\frac{d\sin\hat{\theta}_{\ell}}{c}}, \cdots, e^{-j2\pi(M-1)(f + f_c)\frac{d\sin\hat{\theta}_{\ell}}{c}}\right]^{T}.$$
(6)

B. System Capacity under Beam Squint

Considering the beamforming vector \mathbf{w} designed based on $\mathbf{a}_{\text{ideal}}(\hat{\theta})^1$ and the actual, frequency-dependant, array response $\mathbf{a}(\theta,f)$, the resultant array gain g in an arbitrary direction θ is also frequency dependent, and it is given as

$$g(\theta, f) = \frac{1}{\sqrt{M}} \mathbf{w}^H \mathbf{a}(\theta, f),$$

$$= \frac{1}{\sqrt{M}} \mathbf{a}_{\text{ideal}}(\hat{\theta})^H \mathbf{a}(\theta, f),$$

$$= \frac{1}{\sqrt{M}} \sum_{m=1}^{M} e^{-j2\pi \frac{d}{c}(m-1)\left[(f+f_c)\sin\theta - f_c\sin\theta\right]}.$$
(7)

Using the sum of geometric series formula (i.e., $\sum_t^T b^t = (1-b^{T+1})/(1-b)$) followed with some simplification, (7) can be reduced to

$$g(\theta, f) = \frac{1}{\sqrt{M}} \frac{\sin(\pi x(\theta, f)M)}{\sin(\pi x(\theta, f))} e^{-j\pi x(\theta, f)(M-1)}, \quad (8)$$

where $x(\theta,f)=\frac{d}{c}[(f+f_c)\sin\theta-f_c\sin\hat{\theta}]$. Clearly, $g(\theta,f)$ in (8) is maximum when $x(\theta,f)\to 0$. Conse-

 1 Note that the multipath index ℓ is dropped here and in the subsequent equations just for the sake of notational simplicity.

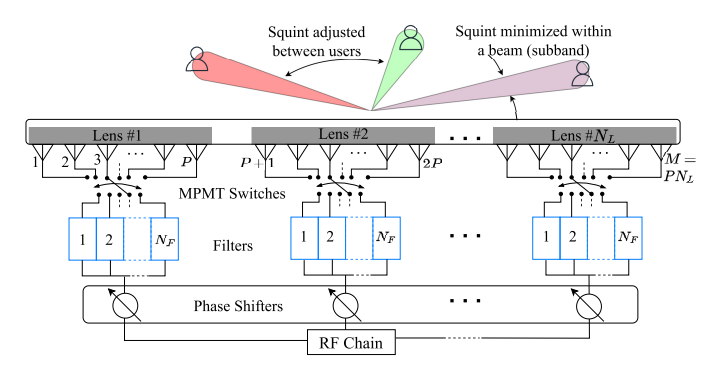


Fig. 2: LAS based mMIMO design for controlling beam squint.

quently, for the k^{th} subcarrier centered at frequency $f_k = ((k-1)-(N-1)/2)\times \Delta f + f_c$ with Δf being the subcarrier spacing, the maximum gain is in

$$\theta_{\text{max}}(f_k) = \sin^{-1}\left(\frac{\sin\hat{\theta}}{1 + f_k/f_c}\right) \tag{9}$$

which does not align with the desired direction $\hat{\theta}$. Therefore, in the presence of the beam squinting effect, a gain loss is incurred in the desired beam direction which leads to capacity degradation. For a system with $N_{\rm RF}$ RF chains operating with bandwidth W under LoS channel and signal-to-noise ratio (SNR) γ , the system capacity is given by

$$C = \frac{W}{N} \sum_{r=1}^{N_{\text{RF}}} \sum_{k=1}^{N} \log_2 \left[1 + \frac{\gamma}{N_{\text{RF}} \frac{W}{N}} |g_r(\hat{\theta}_r, f_{k,r})|^2 \right]. \tag{10}$$

III. THE PROPOSED TECHNIQUE: INTENTIONAL BEAM SQUINT FOR DOWNLINK MULTIPLE ACCESS WITH SINGLE RF CHAIN

In this work, we adopt a modified LAS based mMIMO system, which was initially proposed in [10] for beam squinting mitigation, to create intentionally squinted beams to specific directions of interests. Generally, the LAS systems employ a combination of two beam steering mechanisms, namely, phase shifter (PS) and switching networks, to steer a beam to a desired direction with the main focus of enhancing the field of view (or scan angle) and steering resolution [14]. The adopted modified LAS design, shown in Fig. 2, exploits the said combination of the steering mechanisms along with analog subband filters and multiple pole multiple throw (MPMT) switches to impart full control of the squinted beams in the analog domain. This work leverages this acquired squinted beams control capability to steer them to different directions of interests, rather than steering them back to the original direction. The full process involves two main steps described below:

A. Subbands Generation and User Scheduling

Considering that severity of beam squinting grows gradually from the middle to the edge subcarriers, it is appropriate to consider that the close by subcarriers causes more or less the same amount of squinting. Therefore, the modified LAS design employs a bank of analog subband filters to chunk the wideband signal from the PSs into groups of narrowband

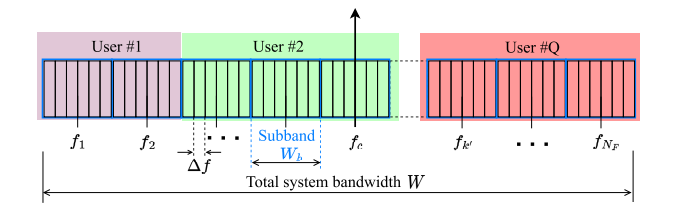


Fig. 3: Visualization of the subbands and user scheduling

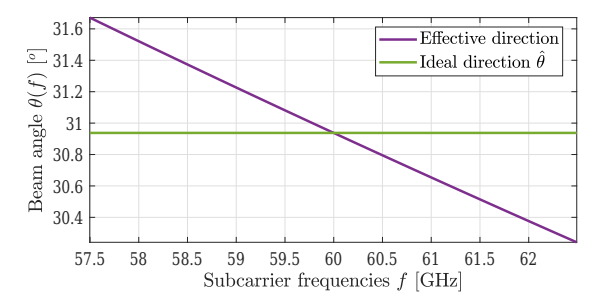


Fig. 4: Relationship between subcarrier frequencies and the resultant beam direction with respect to the ideally desired direction. The figure was plotted with $M=128,\,f_c=60GHz,\,W=5GHz,$ and N=1024

signals such that the maximum squinting within each subband (with respect to the center frequency of that subband) is within a tolerable range. Assuming that the maximum tolerable residual squinting within each subband is not more than a quarter of 3 dB beamwidth Ω_{3dB} , for a given bandwidth W, the optimum number of subbands is given by [10]

$$N_F = \left[\frac{W \sin(\pi/4 - \Omega_{3dB}/8)}{\sqrt{2} f_c \left(1 - \sqrt{2} \sin(\pi/4 - \Omega_{3dB}/8) \right)} \right], \quad (11)$$

where $\Omega_{3\mathrm{dB}} \approx (1.3\lambda)/(Md)$ [15]. Accordingly, size of each subband can be given by $W_b = W/N_F$ and the center frequency of the k' subband is given by $f_{k'} = ((k'-1)-(N_F-1)/2)\times \Delta f + f_c$ where $k'=1,2,\ldots,N_F$. Once the number of subbands is determined, the localized subcarrier mapping is used to map the data of different users on the subcarriers in W, as shown in Fig. 3. The blocks of subcarriers pertained to different users must be aligned with the locations of the subbands. Note that, with N_F subband, the system can serve up to $Q=N_F$ users with each user occupying one subband, where Q is the total number of users. However, depending on the data rate requirement, users may be allocated with a larger block size spanning multiple subsequent subbands (in this case $Q < N_F$).

In order to simplify the beam search process under the lenses (discussed in the subsequent subsection) location of each user's block within W (i.e., the user-to-subband scheduling) must be considered properly. From Fig. 4, plotted using (9), it is clear that subcarriers on the left of the middle subcarrier cause the squinted beams to deviate toward the right side of the original beam direction and vice versa. Accordingly, we schedule the users to the subbands such that the resultant squinted beams are readily oriented toward the directions of the targeted users, which simplifies the process of adjusting directions of these beam toward intended.

Therefore, the scheduling process starts by sorting the users

based on their directions $(\hat{\theta}_q,$ where $q=1,2,\ldots,Q)$, i.e., the required AoDs for each of them, in ascending order with respect to the array's boresight. The middle user in the list is taken as the reference user, its data is scheduled at the midmost subbands and the direction of the main beam is adjusted based on its location. Based on the observation from Fig. 4 discussed above, the rest of the users are scheduled based on their locations with respect to the reference user. The users located on the left of the reference user are scheduled on the right-side subbands and vice versa.

B. RF Precoding and Multi-beams Generation

In this step, the RF precoding technique that aligns the squinted beams to the directions of the target users is described. Initially, the whole signal (of bandwidth W) from the RF chain passes through the PS network where each PS adds a fixed delay to it based on the direction $\hat{\theta}_{q_{\text{ref}}}$ of the reference user. Therefore, the PS precoder, \mathbf{f}_{PS} , is designed as

$$\mathbf{f}_{\text{PS}} = \frac{1}{\sqrt{N_L}} \left[1, e^{j\frac{2\pi d_L}{\lambda_c} \sin \hat{\theta}_{q_{\text{ref}}}}, \cdots, e^{j\frac{2\pi d_L}{\lambda_c} (N_L - 1) \sin \hat{\theta}_{q_{\text{ref}}}} \right]^T \tag{12}$$

where N_L is the number of lens element, $d_L = P \times d$ is the inter-lens distance and P is the number of antenna elements under each lens. After the PSs, the signal is passed through N_L groups of subband filters (each group with N_F filters) to be chunked into subbands, i.e., blocks of narrowband signals intended for different users (as explained in section III-A above). Each narrowband signal passes through the switching mechanism using MPMT switches modeled by a precoder \mathbf{F}_{LAS} to the lenses for transmission. The MPMT switches allow simultaneous activation of N_F (one for each subband) antennas under each lens. The \mathbf{F}_{LAS} precoder is given by

$$\mathbf{F}_{\text{LAS}} = \begin{bmatrix} \mathbf{s}^{(0)} & \mathbf{0}_{P \times 1} & \cdots & \mathbf{0}_{P \times 1} \\ \mathbf{0}_{P \times 1} & \mathbf{s}^{(1)} & & \mathbf{0}_{P \times 1} \\ \vdots & & \ddots & \vdots \\ \mathbf{0}_{P \times 1} & \mathbf{0}_{P \times 1} & \cdots & \mathbf{s}^{(N_L - 1)} \end{bmatrix}, \tag{13}$$

where $\mathbf{s}^{(n)}$ is a $P \times 1$ antenna element selection vector under n^{th} LAS. The p^{th} element in $\mathbf{s}^{(n)}$ activates p^{th} antenna element of the n^{th} LAS for an incoming k'^{th} subband. The p^{th} antenna of n^{th} LAS radiates toward $\theta^{(n)}(p) = \pi/4 - \pi p/(2(P-1))$ [13]. Combination of arbitrary $\theta^{(n)}(p)$'s from all subarrays for k'^{th} subband results into an effective beam direction $\theta_{\text{LAS}}(k')$. Consequently, the effective RF precoder for k'^{th} subband is given by

$$\mathbf{f}_{RF}(k') = \mathbf{F}_{LAS}\mathbf{f}_{PS}.\tag{14}$$

Considering the frequency-dependant array response vector (6) at any effective direction $\theta_{LAS}(k')$, the effective beam gain due to k'^{th} subband can be found as

$$g(\theta_{\text{LAS}}(k'), f_{k'}) = \mathbf{f}_{\text{RF}}^{H}(k') \ \mathbf{a}(\theta_{\text{LAS}}(k'), f_{k'})$$

$$= \frac{1}{\sqrt{N_L P}} \sum_{n=0}^{N_L - 1} \sum_{p=0}^{P - 1} e^{-j2\pi \frac{d}{c} f_c P n \sin \hat{\theta}_{q_{\text{ref}}}}$$

$$\times e^{-j2\pi \frac{d}{c} f_c (\frac{(P - 1)}{2} - p) \sin \theta^{(n)}(p)}$$

$$\times e^{-j2\pi \frac{d}{c} (P n + p) (f_{k'} + f_c) \sin \theta_{\text{LAS}}(k')}.$$
(15)

Then the precoder \mathbf{f}_{RF} seeks to find an optimum set of $\theta^{(n)}(p)$'s, i.e., $\Phi_q^{\text{opt}}(k') = \{\theta^{(1)}, \theta^{(2)}, \dots, \theta^{(n)}, \dots, \theta^{(N_L)}\}$, for all lenses that maximizes the beam gain g toward the effective direction $\theta_{\text{LAS}}^{\text{opt}}(k') \approx \hat{\theta}^{(q)}$ for the k'^{th} subband scheduled for the q^{th} user. To this end, an exhaustive search algorithm can be used to solve for $\Phi_q^{\text{opt}}(k')$ that satisfies

$$\min_{\Phi_q(k')} |\hat{\theta}^{(q)} - \theta_{\text{LAS}}(k')|. \tag{16}$$

Algorithm 1: The proposed beam squint controlling mechanism for multiple access in single RF path.

Input: f_c , \overline{W} , M, users' angles.

Output: $\mathbf{F}_{1\Delta S}^{(\text{opt})}$

- 1 Calculate the optimum number of analog subband filters N_F as specified in (11).
- 2 Build the proposed LAS design for a single RF chain as illustrated in Fig. 2.
- 3 **Sort** users in terms of their angles in ascending order, and assign the middle user in the list to be the reference user that has $\hat{\theta}_{\alpha}$...
- that has $\hat{\theta}_{q_{\text{ref}}}$.

 4 **Adjust** the PS network for beamforming as given in (12) using the angle of the reference user to be the angle of the PSs (i.e., $\theta_{\text{PS}} = \hat{\theta}_{q_{\text{ref}}}$).
- 5 Assign the users to the subbands in descending order, where the last user (q=Q) occupies the first B_Q subbands, and so on.

10 Calculate
$$\mathbf{F}_{\mathrm{LAS}}^{\mathrm{opt}}$$
 as $\mathbf{F}_{\mathrm{LAS}}^{\mathrm{opt}} = \left[\mathbf{F}_{\mathrm{LAS}}^{\mathrm{opt}}(1), \mathbf{F}_{\mathrm{LAS}}^{\mathrm{opt}}(2), \cdots, \mathbf{F}_{\mathrm{LAS}}^{\mathrm{opt}}(k'), \cdots, \mathbf{F}_{\mathrm{LAS}}^{\mathrm{opt}}(N_F) \right]$

C. User and System Capacity

Since there are multiple desired directions under the considered multiuser scenario and the squinted beams are optimized to provide maximum gains toward those directions, the beam gain loss discussed in Section II-B is reclaimed and the overall system capacity is improved. The total system capacity can be obtained as summation of the capacities of the individual users, i.e., $C = \sum_{q=1}^{Q} C_q$, where C_q is the capacity of the q^{th} user, given by

$$C_{q} = \sum_{k'=1}^{B_{q}} \frac{W_{b}}{N'} \sum_{k''=0}^{N'-1} \log_{2} \left[1 + \frac{\gamma N'}{W_{b}} \left| g\left(\theta_{\text{LAS}}^{\text{opt}}(k'), f_{k''|_{k'}}\right) \right|^{2} \right]$$
(17)

where B_q is the total number of subbands assigned to the q^{th} user $\left(\sum_q^Q B_q = N_F\right)$, N' is the total number of subcarriers in each subband, i.e., $N' = W_b/\Delta f$, and $f_{k''|_{k'}}$ is the frequency of the k''^{th} subcarrier within k'^{th} subband of the q^{th} user. Here, it is pertinent to mention that, $\theta_{\rm LAS}^{\rm opt}(k')$ is optimized based on the subband's center frequency $f_{k'}$, thus the other subcarriers at $f_{k''} \neq f_{k'}$ within the subband may still cause some residual squinting. This is taken care of during the design of N_F in (11) as discussed in Section III-A above.

The proposed RF precoding for beam squint-based multiple access is summarized in Algorithm 1.

IV. EXTENSION TO MULTIPLE RF CHAINS

In this section, the above discussed multiple access technique is extended to the case of the full-connected hybrid mMIMO system in which N_{RF} RF chains are utilized. With multiple RF chains, more users can be accessed simultaneously as each RF chain can be used to serve different groups of users, thereby enhancing the overall system capacity. While the RF precoding technique discussed in section III-B is applicable for each RF chain, the groups of users to be served by each RF chain must be properly considered, taking the interference issue into account. Since the subbands resources are reused in each RF chain, users from different RF chains using the same subbands must be spatially orthogonal in order to avoid interference between them. To this end, we adopt the fixed quantization user grouping algorithm [16] to partition the users into N_{RF} spatial groups. This user grouping approach relies on the fact that, for large antenna arrays, channel eigenspaces are approximately mutually orthogonal given that their AoA supports are disjoint [17]. Accordingly, based on the geometry of the user locations and their channel scattering², $N_{\rm RF}$ $\hat{\theta}_{q_{\rm ref}}$'s and angular spread Δ are defined such that the resulting N_{RF} intervals $\left[\hat{ heta}_{q_{\mathrm{ref}}} - \Delta, \hat{ heta}_{q_{\mathrm{ref}}} + \Delta \right]$ form disjoint sectors. Eigenspaces corresponding to these sectors are then computed considering the one-ring scattering model [17]. User groups are formed by associating the users to the computed eigenspaces based on their minimum chordal distance.

Once spatial groups of the users are formed, each group is served by one RF chain, and the user-subband scheduling process within each group is performed as in section III-A.

With the considered full-connected hybrid mMIMO, the precoding step includes analog and digital precoding stages. The analog precoding is responsible for creating the physical beams and controlling their squints while the digital precoding minimizes interference between RF beams pertained to different RF chains. The analog precoder $\mathbf{F}_{RF}(k') \in \mathbb{C}^{M \times N_{RF}}$ for k'^{th} subband for a given RF chain is designed as in section III-B and summarized in Algorithm 1. The digital basesbad precoder $\mathbf{F}_{BB}(k'') \in \mathbb{C}^{N_{RF} \times N_{RF}}$ for k''^{th} subcarrier in the k'^{th} subband is designed based on

$$\min_{\mathbf{F}_{BB}(k'')} \sum_{k'=1}^{N_F} \sum_{k''=1}^{N'} ||\mathbf{F}_{opt}(k'') - \mathbf{F}_{RF}(k')\mathbf{F}_{BB}(k'')||_F^2,$$
 (18)

whose least squares solution can be found as [18]

$$\mathbf{F}_{\mathrm{BB}}(k^{\prime\prime}) = \mathbf{F}_{\mathrm{RF}}^{\dagger}(k^{\prime})\mathbf{F}_{\mathrm{opt}}(k^{\prime\prime}) \tag{19}$$

where $\mathbf{F}_{\text{opt}}(k'')$ is the optimal digital precoder for the k''^{th} subcarrier.

V. NUMERICAL RESULTS AND DISCUSSION

In this section, performance of the proposed design is analyzed in terms of beam gain and capacity. Unless stated

TABLE I: Simulation parameters.

| Parameters | Value |
|--|---------------|
| Operating frequency f_c | 60 GHz |
| System bandwidth W | 5 GHz |
| Channel paths L_p | 1 |
| Antenna elements M | 128 |
| Distance between antenna elements d | $\lambda_c/2$ |
| Number of RF chains N_{RF} | 1,2 |
| Number of subcarrier frequencies N | 2048 |
| Number of lenses N_L | 4 |
| Number of analog subband filters N_F | 16 |
| Number of antenna per lens P | M/N_L |

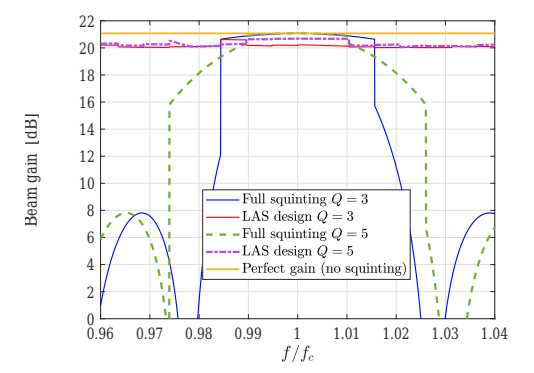


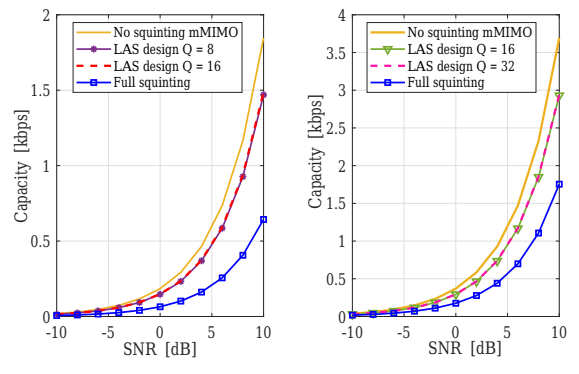
Fig. 5: Beam gain vs normalized frequency.

otherwise, the numerical values of the used system parameters used for simulation are given in Table I. The users are assumed to be uniformly distributed in the spatial domain between $[-\pi/4, \pi/4]$ as $\pm \pi/4$ is maximum scanning range of the LAS systems [13]. Conventional mMIMO systems with and without (i.e., the ideal case) beam squint problems are used as the benchmarks.

Fig. 5 shows typical beam gains performance for different number of users with arbitrary directions, i.e., random θ_q . In the case of Q=3, $\hat{\theta}_q$'s are set as $\{45^o, 10^o, -35^o\}$ and with Q = 5, $\hat{\theta}_q$'s are set as $\{40^o, 20^o, 10^o, -20^o, -30^o\}$. In both cases, the middle angles are selected as the $\hat{\theta}_{q_{\rm ref}}$'s. For fair comparison, we have calculated the subcarrier gains of the "Full Squinting" case (i.e., the blue and green curves) based on the direction of the user to which that is assigned in the proposed approach. It is clear from these curves that with 5 users, the beam gain performance is enhanced, as compared to 3 users case, even without beam squint control mechanism as established in [11]. However, having the ability to control the squinted beams combined with this inherent performance gain with multi users leads to ultimate beam gain performance enhancement as justified by the proposed approach. It is clear from Fig. 5 that the achieved beam gains with the proposed design is only around 1 dB less than that of the perfect ideal system for all subcarriers in both cases.

Fig. 6 presents the overall system capacity as a function of SNR for a different number of users and RF chains. Here, the results are averaged over a random set of users with random directions within the system's scan range specified above. It is clear that the proposed design improves system capacity significantly. It should be noted that, while increasing the number of RF chains enhances the system capacity due to the

²This information can be easily obtained from the user's channel state information (CSI) using uplink pilots. The CSI acquisition process is simplified further by the static/semi-static nature of the mMTC/IoT devices targeted by this work.



(a) Capacity vs SNR ($N_{\rm RF}=1$) (b) Capacity vs SNR ($N_{\rm RF}=2$)

Fig. 6: Overall system capacity performance for different Q and N_{RF} .

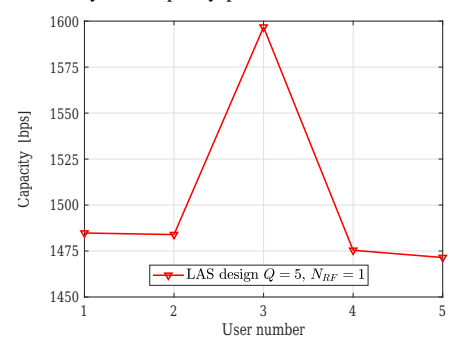


Fig. 7: Typical capacity performance of individual users at SNR = 10 dB.

re-usage of the frequency resources, increasing the number of users within a given RF chain does not. This is mainly because the total bandwidth remains the same within one RF chain and the users share it through frequency-domain multiplexing. However, the proposed design is capable of serving multiple users with moderate to low data rate requirements even with a single RF chain, making it more appealing for IoT and mMTC services.

While Fig. 6 shows the overall system capacity, Fig. 7 shows a typical capacity performance of individual users according to their location with respect to the reference user. It is clear from the figure that the middle user which is taken as the reference user by the proposed system has the best performance. The rationale behind this is simple. The reference user is scheduled to occupy the subbands close to f_c which readily experiences less squinting amount and the direction of the main beam (from PSs) is adjusted based on its location (i.e., $\theta_{q_{\rm ref}}$). As an extension of this work, a better scheduling mechanism that allows the IoT device with stringent performance requirements to be set as the reference user can be developed.

VI. CONCLUSION AND FUTURE DIRECTION

In this paper, a LAS based mMIMO system capable of controlling and exploiting the beam squint phenomenon for serving multiple spatially distributed users is proposed. The RF precoding mechanism that enables the generation of multiple beams with a controlled amount of squint, as well as the user scheduling mechanism, are presented and evaluated. The proposed system was found to improve system gain and

capacity by benefiting from the beam squint phenomenon while allowing the system to serve multiple users even with single RF chain. In this work, an exhaustive search algorithm has been used during the RF precoding, a low-complexity search algorithm with similar performance can be sought in future work. Additionally, a better scheduling algorithm that considers the requirements of individual users will also be developed.

VII. ACKNOWLEDGEMENT

This work was supported in part by the U.S. National Science Foundation under Award ECCS-1923857.

REFERENCES

- [1] S. A. Busari *et al.*, "Millimeter-wave massive MIMO communication for future wireless systems: A survey," *IEEE Commun. Surveys Tuts.*, vol. 20, no. 2, pp. 836–869, 2017.
- [2] D. Cassioli *et al.*, "The ultra-wide bandwidth indoor channel: From statistical model to simulations," *IEEE J. Sel. Areas Commun.*, vol. 20, no. 6, pp. 1247–1257, 2002.
- [3] B. Wang et al., "Spatial-wideband effect in massive MIMO with application in mmWave systems," *IEEE Commun. Magazine*, vol. 56, no. 12, pp. 134–141, 2018.
- [4] Z. Liu et al., "Minimize beam squint solutions for 60Ghz millimeterwave communication system," in Proc. 78th Veh. Technol. Conf. (VTC Fall), Las Vegas, NV, 2013, pp. 1–5.
- [5] M. Cai et al., "Effect of wideband beam squint on codebook design in phased-array wireless systems," in Proc. IEEE Global Commun. Conf. (GLOBECOM), Washington, DC, 2016, pp. 1–6.
- [6] H. Yu et al., "Performance analysis and codebook design for mmWave beamforming system with beam squint," *IEEE Wireless Commun. Lett.*, 2021.
- [7] G. Li et al., "Beam squint compensation for hybrid precoding in millimetre-wave communication systems," *Electron. Lett.*, vol. 54, no. 14, pp. 905–907, 2018.
- [8] J. P. González-Coma, W. Utschick, and L. Castedo, "Hybrid LISA for wideband multiuser millimeter-wave communication systems under beam squint," *IEEE Trans. Wireless Commun.*, vol. 18, no. 2, pp. 1277– 1288, 2019.
- [9] Z. Sattar et al., "Antenna array gain and capacity improvements of ultrawideband millimeter wave systems using a novel analog architecture design," *IEEE Wireless Commun. Lett.*, vol. 9, no. 3, pp. 289–293, 2019.
- [10] L. Afeef, A. B. Kihero, and H. Arslan, "Novel transceiver design in wideband massive MIMO for beam squint minimization," arXiv preprint arXiv. 2022.
- [11] I. Laurinavicius et al., "Beam squint exploitation for linear phased arrays in a mmWave multi-carrier system," in Proc. IEEE Global Commun. Conf. (GLOBECOM), Waikoloa, HI, 2019, pp. 1–6.
- [12] M. Karabacak et al., "Hybrid MIMO architecture using lens arrays," Jul. 14 2020, US Patent 10,714,836.
- [13] ——, "Lens antenna subarrays in mmWave hybrid MIMO systems," IEEE Access, vol. 8, pp. 216 634–216 644, 2020.
- [14] G. Mumcu et al., "Mm-Wave beam steering antenna with reduced hardware complexity using lens antenna subarrays," *IEEE Antennas Wireless Propag. Lett.*, vol. 17, no. 9, pp. 1603–1607, 2018.
- [15] S. Bhattacharyya and G. Aruna, "Radiation pattern analysis of uniform rectangular planar arrays for millimeter wave communications: Comparative study with uniform linear arrays," Wireless Personal Commun., pp. 1–22, 2020.
- [16] J. Nam et al., "Joint spatial division and multiplexing: Opportunistic beamforming, user grouping and simplified downlink scheduling," *IEEE J. Sel. Topics Signal Process.*, vol. 8, no. 5, pp. 876–890, 2014.
- [17] A. Adhikary et al., "Joint spatial division and multiplexing—The large-scale array regime," *IEEE Trans. Inf. Theory*, vol. 59, no. 10, pp. 6441–6463, 2013.
- [18] X. Yu et al., "Alternating minimization algorithms for hybrid precoding in millimeter wave MIMO systems," *IEEE J. Sel. Topics Signal Process.*, vol. 10, no. 3, pp. 485–500, 2016.